http://dx.doi.org/10.5012/bkcs.2014.35.10.2901

One-step Microwave Synthesis of Hierarchical Structured $LiFePO_4$ using Citric Acid

Mihye Wu,* Sungho Choi, Yongku Kang, and Ha-Kyun Jung*

Advanced Materials Division, Korea Research Institute of Chemical Technology, Daejeon 305-343, Korea
**E-mail: wumihye@krict.re.kr (M. Wu); hakyun@krict.re.kr (H.-K. Jung)*
Received March 3, 2014, Accepted June 3, 2014

The hierarchical-structured $LiFePO_4$ cathode materials were synthesized by one-step microwave synthesis, and their electrochemical properties were investigated. Addition of citric acid during the reaction lead to the formation of hierarchical structured $LiFePO_4$, which has both nano- and micron-characteristics advantageous for energy density and electrode fabrication. Adjusting the molar ratio of Fe to citric acid enhanced the electrochemical properties of $LiFePO_4$.

Key Words : Microwave, Hierarchical structure, $LiFePO_4$, Citric acid

Introduction

There are diverse approaches used in preparing electrode materials (*e.g.*, solid-state, sol-gel, co-precipitation, solvothermal, hydrothermal method).[1-8] The electrochemical properties of materials are highly dependent on their method of preparation, so adjusting synthesis methods to be more effective is essential in synthesizing cathode materials.[9] Microwave synthesis has been widely adopted as a useful method for preparing electrode materials. The synthetic route is simple and fast, which is economically and environmentally advantageous, and uniformity can be achieved due to reaction processes occurring at the molecular level.[10-13]

$LiFePO_4$ has been intensively studied as a potential cathode material because of advantages that include excellent thermal stability, good cycleability, low cost, nontoxicity and safety.[14-17] However, one of the main problems with $LiFePO_4$ is that the compound has poor ionic and electrical conductivity.[18-20] Many efforts have been made to overcome this problem, and reducing the particle size to nano-scale is accepted as being one of the most effective ways to improve the ionic and electrical conductivity of the electrode material. Nano-structuring can facilitate lithium-ion diffusion in the electrode materials by shortening the diffusion lengths for lithium ions.[21] The electrical conductivity of nano-structured materials can be effectively enhanced by providing short path-lengths for electronic transport.[22] Moreover, greater contact area increases the accessibility of electrolyte, leading to high power performance.[23]

Despite these advantages based on the nano-structuring, there are still disadvantages. Nano-sized materials show lower density comparing with micron-sized materials, which leads to lower energy density of the electrode, and limits the total volumetric energy density of lithium-ion batteries. To enhance the strength and make up for the weakness, some solutions (*i.e.*, fabricating nano/nano-mixed or nano/micro-mixed electrode materials) have been suggested.

In this work, we successively synthesized hierarchical structured $LiFePO_4$, composed of micron-sized particles formed by the nano-sized primary particles by one-step microwave synthesis using citric acid. The hierarchical structuring enables the electrode material to have both nano- and micron-characteristics. Nano-sized primary particles of $LiFePO_4$ can be kinetically and thermodynamically favorable; while micron-sized particles can increase the pack density so that the total volumetric energy density of lithium-ion batteries can be increased. The effect of citric acid on synthesizing hierarchical structured $LiFePO_4$ and the electrochemical performance of the material was investigated.

Experimental

Preparation of $LiFePO_4$. $LiFePO_4$ was prepared by a one-step microwave synthesis using lithium acetate dihydrate (Sigma-Aldrich, reagent grade), iron(II) sulfate heptahydrate (Sigma-Aldrich, 99.0%), ammonium phosphate monobasic (Sigma-Aldrich, 99.99%), sucrose (Fluka, 99.0%), methacrylic acid (Aldrich, 99.0%) and citric acid monohydrate (DAE JUNG chemicals, 99.5%) as raw materials. All the chemicals were used without further purification.The molar ratio of the Li:Fe:P was 3:1:2. The proper amount of sucrose and methacrylic acid was 15 and 30 wt % of the calculated final product, respectively. The molar ratios of Fe to citric acid were 1:0, 1:0.8, 1:1, 1:1.2, 1:1.4, and 1:1.6. Polyvinylpyrrolidone (PVP) with a molecular weight of 10,000 was dissolved in deionized water resulting in a 25% w/w solution. This solution was then added to the appropriately weighed raw materials. The resultant mixture was transferred and sealed in a Teflon vessel; then placed in a microwave reactor (Model MARS6, CEM Corp., USA). The reaction temperature was raised to 170 ^{o}C, maintained for 15 min; then cooled down to room temperature.

Measurements. The crystal structures were analyzed with a powder diffractometer (Rigaku Ultima IV Diffractometer) with graphite-monochromator equipped with Cu Kα radiation; operating at 40 kV and 40 mA. The particle size and morphology were observed using field-emission scanning electron microscopy (FE-SEM, Tescan Mira 3 LMU FEG,

20 kV).

The cathode was formulated by mixing $LiFePO_4$ powder, super P, and PVdF in a weight ratio of 7:2:1; dispersed in *N*-methylpyrrolidone (NMP). The obtained slurry was spread on Al foil as a current collector, followed by vacuum drying at 120 °C for 12 h. The electrolyte was 1 M $LiPF_6$ dissolved in a mixture of ethylene carbonate/dimethyl carbonate (EC/DMC 1:1, v/v). Li foil was used as a negative electrode, and coin cells (CR2032 type) were assembled in an argon-filled glove box.

Galvanostatic charge/discharge characteristics were measured between 1.5 and 4.5 V at a constant current of 0.1C (17 mA/g) and 1C (170 mA/g). The galvanostatic intermittent titration technique (GITT) was employed at a current pulse of 17 mAh/g for 10 min. The current was turned off for 50 min between each pulse.[24]

The Brunauer-Emmett-Teller (BET) surface area was measured by nitrogen adsorption/desorption at 77.3 K. Before measurement, all the samples were degassed for 30 min at 90 °C, and evacuated for 4 h at 200 °C.

Electrochemical impedance spectroscopy (EIS) was carried out using an impedance analyzer (Bio-Logic) with a frequency range from 10^5 to 0.1 Hz at an amplitude of 10 mV. The impedance spectra were normalized by the active mass of the electrode.[25,26]

Results and Discussion

The XRD patterns for the $LiFePO_4$ synthesized with various ratios of Fe to citric acid are shown in Figure 1. The experimental molar ratios of Fe to citric acid were 1:0, 1:0.8, 1:1, 1:1.2, 1:1.4 and 1:1.6, and we refer to products from these ratios as $LiFePO_4$/CAX, where X represents the molar ratio of citric acid to Fe. As indicated all the patterns except $LiFePO_4$/CA0 were indexed on the orthorhombic structure with space group *Pnma* (JCPDS 97-018-1341), and $LiFePO_4$/CA0 with *Pmnb* (JCPDS 00-042-1499). The synthesized $LiFePO_4$ was well crystallized without any detectable impurity phases despite using citric acid in the one-step microwave reaction.

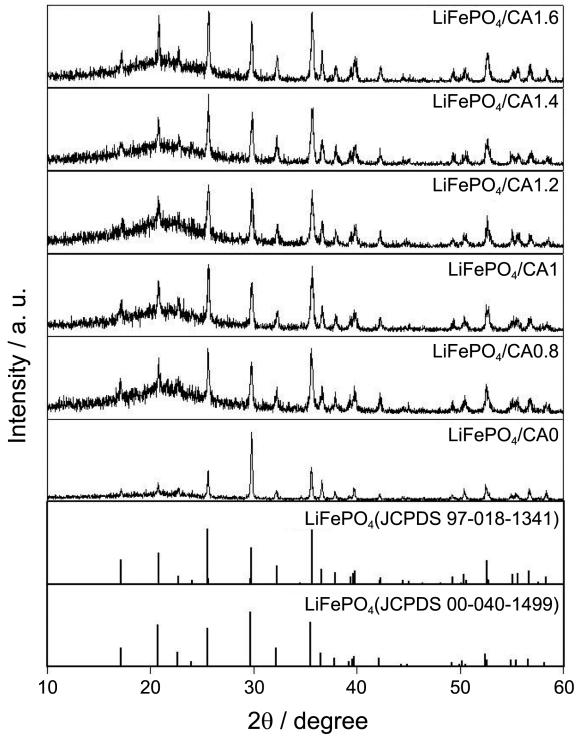

Figure 1. XRD patterns for the $LiFePO_4$ synthesized with various ratios of Fe to citric acid.

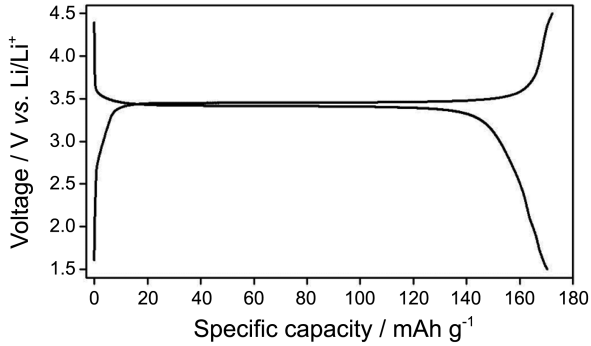

Figure 2. Charge and discharge profiles of $LiFePO_4$/CA1.2 at 0.1C (17 mAh/g).

Figure 2 shows charge and discharge profiles of $LiFePO_4$/CA1.2. The long flat charge and discharge curves were obtained at a potential of about 3.4 V *vs.* Li/Li^+ at 0.1C (17 mA/g), which is related to the two phase redox reaction ($LiFePO_4 \leftrightarrow (1-x)LiFePO_4 + xFePO_4 + xLi^+ + xe^-$).[27] The synthesized $LiFePO_4$/CA1.2 had a discharge capacity of 170 mAh/g, same as its theoretical capacity based on a one-electron reaction.[28] This result shows that the reactivity of the participating lithium ions was very high, and the electrons for the redox reaction were very active. This follows from the fact that the electrochemical reaction of the synthesized $LiFePO_4$ was highly reversible.

Field-emission scanning electron microscopy (FE-SEM) images of $LiFePO_4$ are shown in Figure 3. Figure 3(a) reveals that $LiFePO_4$/CA0 synthesized without citric acid has thick-rod morphology several microns in size; without formation of hierarchical structure. However, the particle morphology changed significantly after adding citric acid for the microwave reaction. Regardless of the molar ratios of Fe to citric acid, all the particles synthesized with citric acid show hierarchical-structure morphology with primary particles of nanorods with a diameter of 20 nm and length of under 400 nm (Figure 3(c), (e), (g), (i), (k)), and hierarchical particles of spherical shape with a diameter of several microns (Figure 3(b), (d), (f), (h), (j)). Moreover, the size of primary particles varies with the molar ratios of Fe to citric acid. The size of nonorods increased with increasing citric acid content. The length of nanorods for $LiFePO_4$/CA0.8 is ranging from 50 to 200 nm, whereas that for $LiFePO_4$/CA1.6 is from 200 to 400 nm, which was grown much longer as the citric acid content increased. The variation in primary particle size influences the diffusion length of lithium ion that can affect the performances of the electrode materials. To investigate

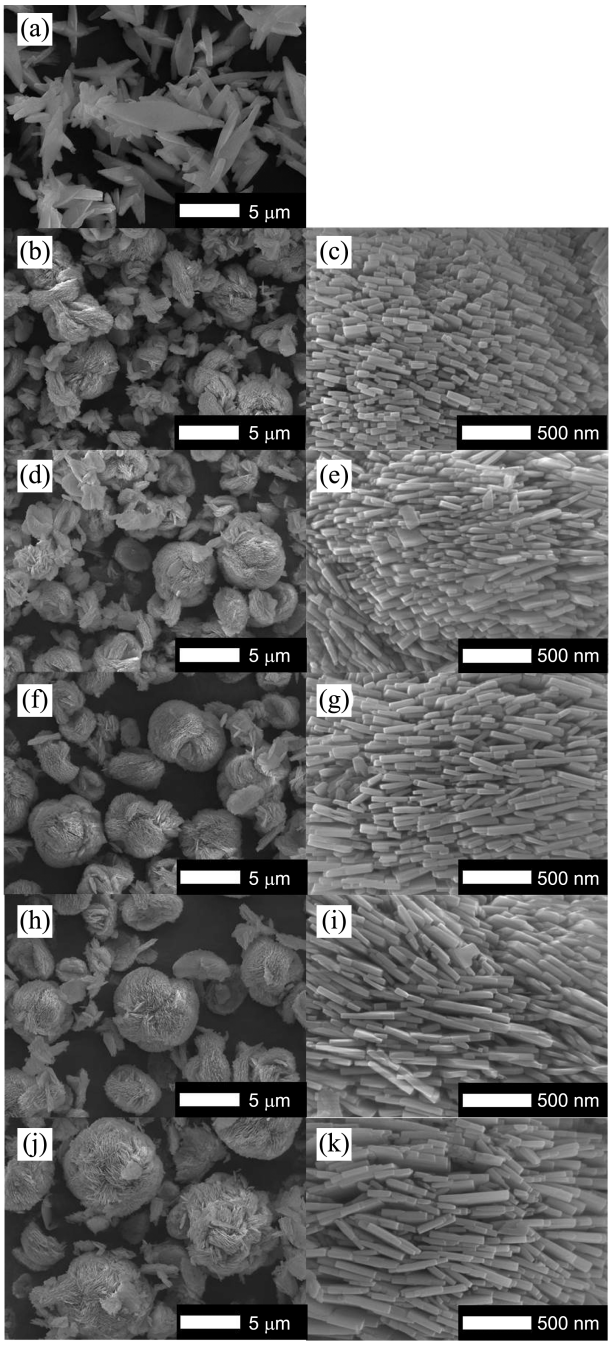

Figure 3. FE-SEM images of $LiFePO_4$: (a) $LiFePO_4$/CA0; (b, c) $LiFePO_4$/CA0.8; (d, e) $LiFePO_4$/CA1; (f, g) $LiFePO_4$/CA1.2; (h, i) $LiFePO_4$/CA1.4; (j, k) $LiFePO_4$/CA1.6.

the differences of the synthesized $LiFePO_4$ according to the primary particle size, Brunauer-Emmett-Teller (BET) techniques were employed. The calculated surface areas were listed in Table 1. A remarkable decrease in the BET surface area was measured for $LiFePO_4$/CA0 compared with other products prepared by adding citric acid. The BET surface area of $LiFePO_4$/CA1.2 was 23.17 m^2/g which was about 12 times higher than that of $LiFePO_4$/CA0, 1.96 m^2/g. This shows that the greater surface area originated in the hierarchical-structure morphology with primary particles of

Table 1. BET surface area

Sample	Specific surface area (m^2/g)
$LiFePO_4$/CA0	1.96
$LiFePO_4$/CA0.8	19.64
$LiFePO_4$/CA1	19.22
$LiFePO_4$/CA1.2	23.17
$LiFePO_4$/CA1.4	20.01
$LiFePO_4$/CA1.6	22.15

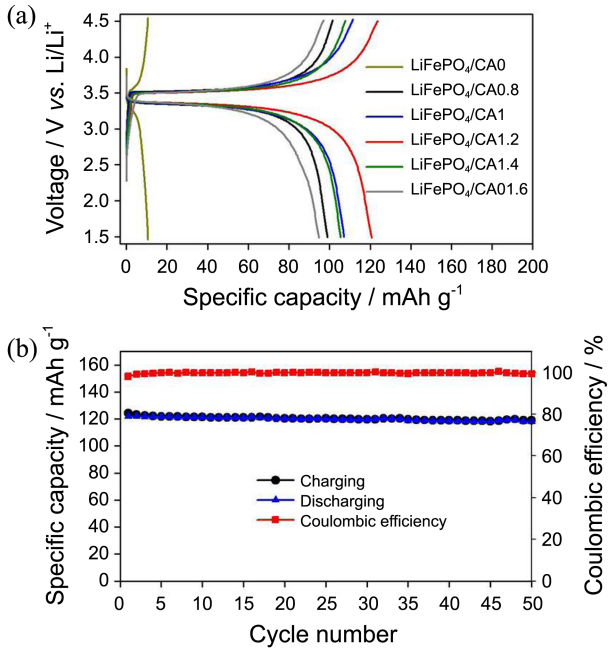

Figure 4 (a) Charge and discharge curves of $LiFePO_4$ synthesized with different molar ratios of Fe to citric acid at 1C, and (b) cycleability and coulombic efficiency of $LiFePO_4$/CA1.2.

nanorods. In addition, there were differences in surface area of citric acid added products in accordance with primary particle size. The $LiFePO_4$/CA1.2 exhibited the highest surface area among other products. Therefore, it is obvious that citric acid addition played a key role in the formation of the hierarchical structure of $LiFePO_4$, and the optimum molar ratio of Fe to citric acid for the highest surface area was 1:1.2.

The nano-sized primary particles can provide advantageous electrochemical factors such as shortening the diffusion and electron transport paths, good electrolyte accessibility, increasing reaction sites, and improving cycling performance. The mi cron characteristics of the particles can offer solutions for low volumetric energy density and electrode fabrication problems. To identify the electrochemical properties in respect of morphologies and surface areas, the charge and discharge curves of $LiFePO_4$ synthesized with different molar ratios of Fe to citric acid at 1C are depicted in Figure 4(a). There are noticeable differences of capacity according to the citric acid addition. The discharge capacity of $LiFePO_4$/CA0 was 11 mAh/g, whereas the citric acid added materials

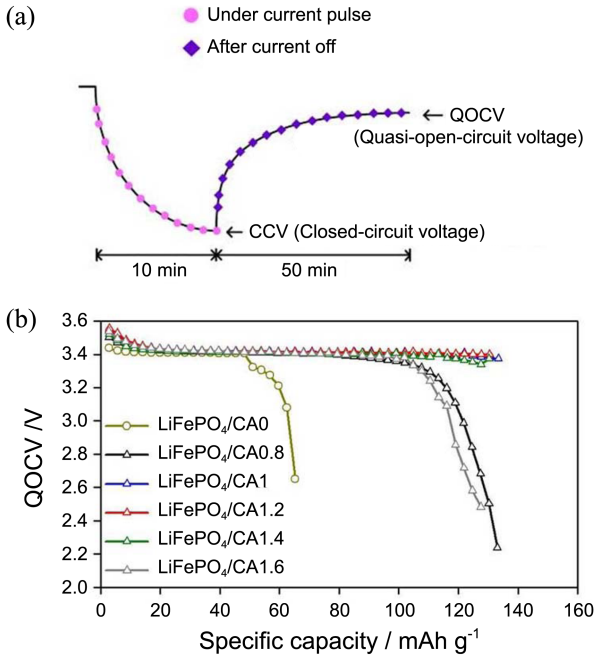

Figure 5. (a) Typical voltage transient in the discharging period and (b) QOCV profiles as a function of discharging capacity.

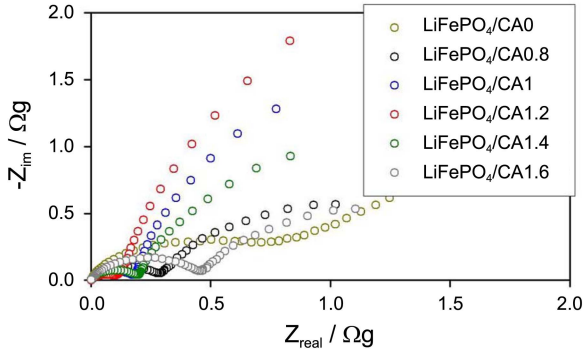

Figure 6. Nyquist plots of $LiFePO_4$ at different molar ratios of Fe to citric acid.

Table 2. EIS parameters of $LiFePO_4$

Sample	R_Ω (Ωg)	R_{ct} (Ωg)
$LiFePO_4$/CA0	1.85×10^{-3}	0.65
$LiFePO_4$/CA0.8	1.29×10^{-3}	0.28
$LiFePO_4$/CA1	0.75×10^{-3}	0.18
$LiFePO_4$/CA1.2	0.74×10^{-3}	0.09
$LiFePO_4$/CA1.4	0.89×10^{-3}	0.19
$LiFePO_4$/CA1.6	1.55×10^{-3}	0.45

showed 100, 107, 121, 106 and 95 mAh/g for $LiFePO_4$/CA0.8, $LiFePO_4$/CA1, $LiFePO_4$/CA1.2, $LiFePO_4$/CA1.4, and $LiFePO_4$/CA1.6, respectively. This dependence of capacity on the inclusion of citric acid is consistent with the FE-SEM and BET results. $LiFePO_4$/CA0 has only micron characteristics; while the others have not only micron characteristics in their hierarchical morphologies, but also nano characteristics in their primary morphologies. Therefore, it is evident that $LiFePO_4$ products with citric acid show higher discharge capacity than those synthesized without citric acid. Also, $LiFePO_4$/CA1.2 exhibits charge and discharge capacities of 124 and 121 mAh/g; which is the optimum condition for this material preparation that having highest surface area of those synthesized $LiFePO_4$. Figure 4(b) shows the cycling performance and coulombic efficiency of $LiFePO_4$/CA1.2 at 1C. As can be seen, the $LiFePO_4$ exhibits a very stable cycling performance with capacity retention of 98% and coulombic efficiency of 99%; after 50 cycles.

To clarify the electrochemical differences of the synthesized products under minimized kinetic effect, QOCV profiles were obtained by the galvanostatic, intermittent-titration technique (GITT).[29,30] The technique was carried out by applying a current pulse for 10 min to the cells to reach the closed-circuit voltage (CCV); followed by a relaxation step of 50 min so that the voltage reached a quasi-equilibrium value (quasi-open-circuit voltage, QOCV - see Figure 5(a)).[31,32] Charging and discharging was continued until the potential of the cell was charged to 4.5 V and discharged to 1.5 V, respectively. Figure 5(b) shows QOCV profiles as a function of the discharge capacity; showing hysteresis at the start and end of the discharge region associated with the citric acid content. At the same QOCV, the various $LiFePO_4$ products exhibited different discharge capacity; indicating that the electrochemical reaction process is different from the citric content. $LiFePO_4$/CA1.2 showed the highest discharge capacity at the same QOCV, $LiFePO_4$/CA0 showed the lowest, and others follows the same tendency toward specific capacity at 1C presented in Figure 4. Therefore, it can be inferred that $LiFePO_4$/CA1.2 is the most favorable thermodynamically, and that $LiFePO_4$/CA0 is least favorable; compared to all the others.

To demonstrate the influence of citric acid addition on kinetics, electrochemical impedance spectroscopy (EIS) was used. The EIS measurement provides information about the internal resistance of electrochemical systems. Nyquist plots of $LiFePO_4$ at different molar ratios of Fe to citric acid are shown in Figure 6, and the fitting results are listed in Table 2. The R_Ω is the total ohmic resistance of the cell; comprising electric conductivity of the electrolyte, separator, and electrodes. The R_{ct} represents the faradic charge-transfer resistance for the electrode reaction; that shows the reaction kinetics.[33] As listed in Table 2, R_Ω is invariant regardless of citric acid ratios. The R_{ct}; however, showed noticeable differences according to the citric acid ratios. Most significantly, $LiFePO_4$/CA0 showed the highest R_{ct} among those synthesized by adding citric acid; a value which was about seven times higher than $LiFePO_4$/CA1.2 (lowest R_{ct}). From this, it can be deduced that the improved electrochemical properties of $LiFePO_4$/CA1.2 originated from its low R_{ct}.

Conclusion

In summary, hierarchical-structured $LiFePO_4$ as a cathode material was fabricated by one-step microwave synthesis.

Adding citric acid is essential in the formation of hierarchical structures, which provide advantages for volumetric energy density and electrode fabrication. The optimum molar ratio of Fe to citric acid for the highest surface area was 1:1.2. The $LiFePO_4$ showed discharge capacity of 170 mAh/g at 0.1C (same as theoretical capacity), and 120 mAh/g at 1C.

Acknowledgments. This work was financially supported by grants from the Fundamental R&D Program for Core Technology of Materials by the Ministry of Knowledge Economy, and the Government-Funded General Research & Development Program by the Ministry of Trade, Industry and Energy, Republic of Korea.

References

1. Andersson, A. S.; Kalska, B.; Häggström, L.; Thomas, J. O. *Solid State Ionics* **2000**, *130*, 41.
2. Prosini, P. P.; Carewska, M.; Scaccia, S.; Wisniewski, P.; Pasquali, M. *Electrochim. Acta* **2003**, *48*, 4205.
3. Arnold, G.; Garche, J.; Hemmer, R.; Ströbele, S.; Vogler, C.; Wohlfahrt-Mehrens, M. *J. Power Sources* **2003**, *119*, 247.
4. Yang, H.; Wu, X.-L.; Cao, M.-H.; Guo, Y.-G. *J. Phys. Chem. C* **2009**, *113*, 3345.
5. Yang, S.; Zhou, X.; Zhang, J.; Liu, Z. *J. Mater. Chem.* **2010**, *20*, 8086.
6. Ellis, B.; Kan, W. H.; Makahnouk, W. R. M.; Nazar, L. F. *J. Mater. Chem.* **2007**, *17*, 3248.
7. Liu, H.; Wu, Y. P.; Rahm, E.; Holze, R.; Wu, H. Q. *J. Solid State Eletrochem.* **2004**, *8*, 450.
8. Dokko, K.; Koizumi, S.; Nakanob, H.; Kanamura, K. *J. Mater. Chem.* **2007**, *17*, 4803.
9. Yang, G.; Ji, H.; Liu, H.; Huo, K.; Fu, J.; Chu, P. K. *J. Nanosci. Nanotechnol.* **2010**, *10*, 980.
10. Wang, L.; Huang, Y.; Jiang, R.; Jia, D. *Electrochim. Acta* **2007**, *52*, 6778.
11. Song, M.-S.; Kim, D.-Y.; Kang, Y.-M.; Kim, Y.-I.; Lee, J.-Y.; Kwon, H.-S. *J. Power Sources* **2008**, *180*, 546.
12. Bilecka, I.; Niederberger, M. *Nanoscale* **2010**, *2*, 1358.
13. Zhang, Y.; Feng, H.; Wu, X.; Wang, L.; Zhang, A.; Xia, T.; Dong, H.; Liu, M. *Electrochim. Acta* **2009**, *54*, 3206.
14. Li, Z.; Zhang, D.; Yang, F. *J. Mater. Sci.* **2009**, *44*, 2435.
15. Chen, Z.; Zhu, H.; Ji, S.; Fakir, R.; Linkov, V. *Solid State Ionics* **2008**, *179*, 1810.
16. Guo, H.; Xiang, K.; Cao, X.; Li, X.; Wang, Z.; Li, L. *Trans. Nonferrous Met. Soc. China* **2009**, *19*, 166.
17. Zhou, W.; He, W.; Li, Z.; Zhao, H.; Yan, S. *J. Solid State Electrochem.* **2009**, *13*, 1819.
18. Hsu, K.-F.; Tsay, S.-Y.; Hwang, B.-J. *J. Mater. Chem.* **2004**, *14*, 2690.
19. Kim, J.-K.; Choi, J.-W., Chauhan, G. S.; Ahn, J.-H.; Hwang, G.-C.; Choi, J.-B.; Ahn, H.-J. *Electrochim. Acta* **2008**, *53*, 8258.
20. Muraliganth, T.; Murugan, A. V.; Manthiram, A. *J. Mater. Chem.* **2008**, *18*, 5661.
21. Wang, Y.; Li, H.; He, P.; Hosono, E.; Zhou, H. *Nanoscale* **2010**, *2*, 1294.
22. Aricò, A. S.; Bruce, P.; Scrosati, B.; Tarascon, J.-M.; Schalkwijk, W. V. *Nature Mater.* **2005**, *4*, 366.
23. Jiang, C.; Hosono, E.; Zhou, H. *Nanotoday* **2006**, *1*, 28.
24. Rui, X. H.; Ding, N.; Liu, J.; Li, C.; Chen, C. H. *Electrochim. Acta* **2010**, *55*, 2384.
25. Alcántara, R.; Ortiz, G. F.; Lavela, P.; Tirado, J. L.; Jaegermann, W.; Thißen, A. *J. Electroanal. Chem.* **2005**, *584*, 147.
26. Chae, O. B.; Park, S.; Ryu, J. H.; Oh, S. M. *J. Electrochem. Soc.* **2013**, *160*, A11.
27. Yang, J.; Xu, J. J. *Electrochem. Solid-State Lett.* **2004**, *7*, A515.
28. Yamada, A.; Chung, S. C.; Hinokuma, K. *J. Electrochem. Soc.* **2001**, *148*, A224.
29. Arai, H.; Okada, S.; Sakurai, Y.; Yamaki, J. *Solid State Ionics* **1997**, *95*, 275.
30. Plashnitsa, L. S.; Kobayashi, E.; Noguchi, Y.; Okada, S.; Yamaki, J. *J. Electrochem. Soc.* **2010**, *157*, A536.
31. Kim, J. W.; Ryu, J. H.; Lee, K. T.; Oh, S. M. *J. Power Sources* **2005**, *147*, 227.
32. Ryu, J. H.; Kim, J. W.; Sung, Y.-E.; Oh, S. M. *Electrochem. Solid-State Lett.* **2004**, *7*, A306.
33. Zhang, S. S.; Xu, K.; Jow, T. R. *Electrochim. Acta* **2004**, *49*, 1057.